PHYSICAL REVIEW A **72**, 032502 (2005)

State-selective detection of near-dissociation ultracold KRb $X\,^1\Sigma^+$ and $a\,^3\Sigma^+$ molecules

D. Wang, E. E. Eyler, P. L. Gould, and W. C. Stwalley
Physics Department, University of Connecticut, Storrs, Connecticut 06269-3046, USA

(Received 21 April 2005; published 13 September 2005)

We report on the state-selective detection of near-dissociation ultracold KRb molecules in the ground $X\,^1\Sigma^+$ state and the metastable $a\,^3\Sigma^+$ state. The molecules are produced by photoassociation of ultracold atoms followed by radiative decay into high vibrational levels of the X and a states. Detection utilizes resonance-enhanced one-color two-photon ionization, followed by time-of-flight mass spectroscopy. Scanning the detection laser frequency over the range 582–625 nm, we observe transitions from the $v''=86-92$ levels of the X state, which are bound by up to 30 cm^{-1}, and the $v''=17-23$ levels of the a state, which are also bound by up to 30 cm^{-1}. The measured vibrational spacings are in excellent agreement with those previously measured and those calculated from the relevant potential curves. Relative vibrational populations are also consistent with Franck-Condon factors for decay from the photoassociated levels.

DOI: 10.1103/PhysRevA.72.032502 PACS number(s): 33.20.Kf, 33.80.Ps, 33.80.Rv, 33.70.Ca

I. INTRODUCTION

Following in the footsteps of ultracold atoms, the area of ultracold molecules has developed rapidly in recent years [1–3]. Polar molecules, with their permanent electric dipole moments, have drawn particular attention [4]. The dipole moments of these heteronuclear molecules allow manipulation with applied electric fields. Because the dipole-dipole potential is both long range and anisotropic, interactions between polar molecules are fundamentally different from those in homonuclear systems. Potential applications include novel quantum degenerate systems [5–11], quantum computation [12], and tests of fundamental symmetries [13]. Investigations of collisions and reactions at these extremely low temperatures also promise to open new areas of ultracold chemistry [14–16].

The technique of ultracold atom photoassociation (PA) [17] has been the primary means for producing molecules at translational temperatures below 1 mK [2]. In this process, laser light resonantly binds two colliding atoms into an excited molecule which subsequently decays by spontaneous emission. This method has recently been successfully adapted to heteronuclear systems [18–26]. Feshbach resonances have been used to make homonuclear molecules at even lower temperatures [27–36], in some cases under quantum degenerate conditions. Based on recent observations of Feshbach resonances in heteronuclear systems [37,38], it can be expected that this route will also yield ultracold heteronuclear molecules in due course. Both PA and Feshbach resonances tend to produce molecules in high vibrational levels with outer turning points at long range. Although these high-v'' states are of interest for some studies, many applications require low-v'' states, because of their improved stability against inelastic processes and their larger dipole moments. Various schemes for populating low-v'' states have been proposed [9,12,20,39–41], and some successful implementations have been reported [19,42].

Direct detection of ultracold molecules has generally utilized photoionization combined with time-of-flight mass spectroscopy. State selectivity is essential to many applications and for diagnosing transfer of population. For example, measuring the v'' dependence of vibrational quenching rates due to collisions with ultracold atoms would be an important first step in studying ultracold molecule collisions. To date, the ability to unambiguously identify the vibrational state of ultracold molecules has been limited, particularly for levels near dissociation. Two-photon one-color ionization spectra have been reported in Rb_2 [43–45], but definitive assignments and initial state identifications were not made. We have recently demonstrated state-selective detection of Rb_2, details of which will be reported elsewhere [46]. In Cs_2, ultracold molecule detection spectra have been compared to absorption measurements, revealing the role of the diffuse bands in the detection process [47]. In K_2, two-photon two-color ionization spectra enabled some identification of the low-v'' states produced by both one-photon [48] and two-photon [42] PA. Dissociation with a separate cw laser helped to clarify the assignment [42]. In Na_2, high-resolution cw ionization spectroscopy yielded clear identification of the highest-lying bound and quasibound rovibrational-hyperfine states [49].

To date, the only heteronuclear system in which state selectivity has been achieved is RbCs. Using two-photon two-color ionization, ultracold molecules were detected in specific vibrational levels of the $a\,^3\Sigma^+$ state [18,20]. In addition, these molecules have been transferred by stimulated emission pumping to the $X\,^1\Sigma^+$ state ($v''=0,1$) and detected in these states with vibrational selectivity [19].

In the present work, we report on vibrationally state-selective detection of ultracold KRb molecules in high-v'' levels of both the ground $X\,^1\Sigma^+$ state and the metastable $a\,^3\Sigma^+$ state. These molecules are formed by cold-atom photoassociation followed by radiative decay, as shown in Fig. 1. Two-photon one-color ionization proceeds through resonant intermediate levels of the $4\,^1\Sigma^+$, $5\,^1\Sigma^+$, $4\,^3\Sigma^+$, and $3\,^3\Pi$ states, allowing vibrational state identification and determination of the relative populations. Using wavelengths in the range of 582–625 nm, we have observed vibrational levels $v''=86-92$ for the X state and $v''=17-23$ for the a state. We have also analyzed spectroscopy of the excited states, details of which will be reported elsewhere [50].

©2005 The American Physical Society

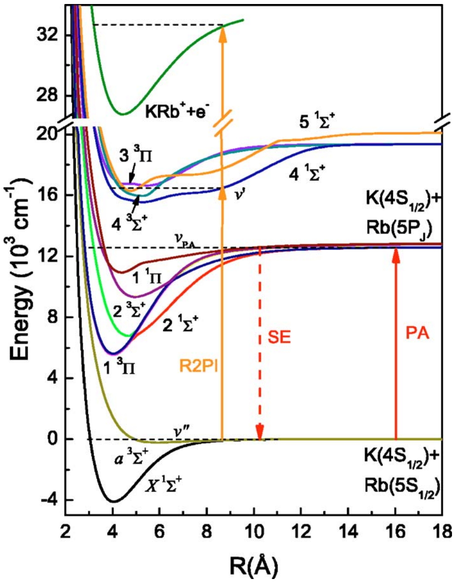

FIG. 1. (Color online) Relevant KRb potential energy curves from [51]. A pair of colliding ground-state atoms is photoassociated (PA) to a bound level v_{PA} below the K$(4S)$+Rb$(5P)$ asymptote which subsequently undergoes spontaneous emission (SE) to either the $X\ ^1\Sigma^+$ or the $a\ ^3\Sigma^+$ state. These states are detected by resonant two-photon ionization (R2PI) through the $4\ ^1\Sigma^+$ and $5\ ^1\Sigma^+$ states (for singlet molecules) or the $4\ ^3\Sigma^+$ and $3\ ^3\Pi$ states (for triplet molecules).

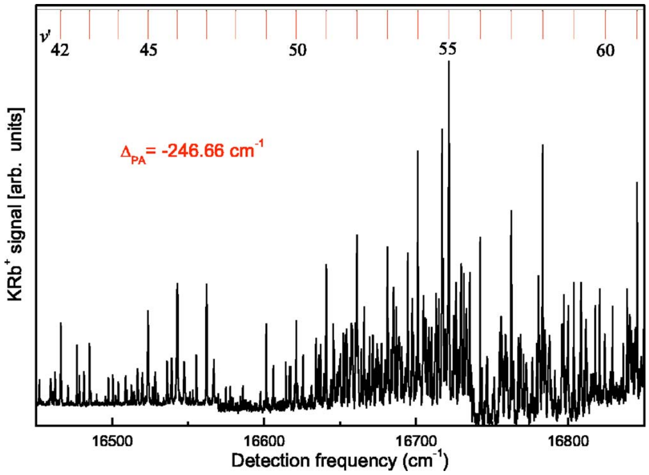

FIG. 2. (Color online) Detection spectrum for singlet molecules. The KRb$^+$ ion signal is plotted as a function of the detection laser frequency. The PA laser is tuned to a $3(0^+)$ $(J=1)$ level at 12 569.94 cm^{-1}, which corresponds to a detuning of -246.66 cm^{-1} below the K$(4S)$+Rb$(5P_{3/2})$ asymptote. Each group of lines is labeled according to the v' level of the $4\ ^1\Sigma^+$ state which is excited. The strongest line in each group corresponds to a transition from $v''=89$ to the v' indicated. The blue end of the spectrum becomes congested and is not yet assigned.

II. EXPERIMENT

Details of the experimental setup have been described previously [25,26]. Here we recount it briefly, focusing on the ionization detection. The KRb PA takes place in overlapping clouds of ultracold ^{39}K and ^{85}Rb. High atomic densities, estimated at 3×10^{10} cm^{-3} for K and 1×10^{11} cm^{-3} for Rb, are achieved using "dark-SPOT" magneto-optical traps (MOTs) for each species. Temperatures for K and Rb of 300 μK and 100 μK, respectively, are expected.

The PA process is driven with a cw tunable titanium-sapphire laser (Coherent 899-29). Its output, typically $>$400 mW, is focused into the overlapping MOT clouds. PA spectra, as described previously [25,26], are obtained by scanning this laser and measuring the ionization signal from molecules which have radiatively decayed into the $X\ ^1\Sigma^+$ ground state and the metastable $a\ ^3\Sigma^+$ state.

In our earlier work [25,26], the ionization detection used a pulsed laser with a broader linewidth and significant amplified spontaneous emission. This prevented state-selective detection but had the benefit of yielding at least some ion signal at most wavelengths, thereby facilitating the location of PA resonances.

In the present work, ionization detection is achieved with a pulsed dye laser (Continuum ND6000) pumped by a frequency-doubled neodymium-doped yttrium aluminum garnet (Nd:YAG) laser at a 10 Hz repetition rate. The use of two dyes, R610 and DCM, provides spectral coverage over the range 582 to 625 nm. The 0.05 cm^{-1} linewidth of the dye laser is sufficient to resolve the vibrational structure, but not the rotational structure, of transitions from levels of the $X\ ^1\Sigma^+$ and $a\ ^3\Sigma^+$ states. This detection laser, with a pulse width of 7 ns and a typical output power of 3 mJ, is focused to a diameter of 1 mm. This is significantly larger than the 0.3 mm diameter of the MOT clouds in order to illuminate a larger fraction of the ballistically expanding cloud of cold molecules. Ions from the laser pulse are accelerated to a channeltron ion detector. KRb$^+$ is discriminated from other species (K$^+$,Rb$^+$,Rb$_2^+$) by its time of flight (TOF).

III. DETECTION SPECTRA FOR SINGLET MOLECULES

Detection spectra are obtained by fixing the PA frequency on a resonance and recording the KRb$^+$ ion signal while scanning the pulsed laser. A 400 cm^{-1} scan for $X\ ^1\Sigma^+$ state molecules is shown in Fig. 2. The spectra display structure on two scales. On a gross scale ($\sim$20 cm^{-1}), nearly periodic spacings correspond to vibrational levels of the upper state of the detection transition, specifically the $4\ ^1\Sigma^+$ state for the spectrum shown in Fig. 2. The spectroscopy of this upper state will be described separately [50]. Measured level spacings and the range of levels observed are both in very good agreement with calculations based on *ab initio* potentials [51]. We note that the increased complexity of the spectrum at higher frequencies is likely due to the appearance of transitions to the $5\ ^1\Sigma^+$ state, which are not yet assigned.

On a finer scale ($\sim$5 cm^{-1}), the structure corresponds to the spacings between high-lying vibrational levels of the $X\ ^1\Sigma^+$ ground state. Specific X-state levels are assigned by matching the measured spacings with those calculated from the potential [52]. Examples are shown in Fig. 3 for PA to two different vibrational levels of the $3(0^+)$ state. As can be seen, the agreement between measured and predicted vibrational spacings is excellent, allowing unambiguous identifi-

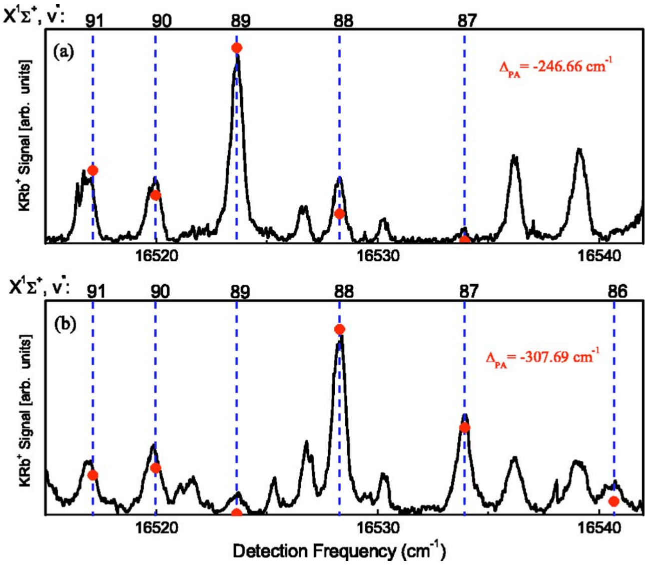

FIG. 3. (Color online) An expanded view of the $v'=45$ group of lines in the singlet detection spectrum for two different $3(0^+)$ PA detunings: (a) -246.66 and (b) $-307.69\ \mathrm{cm}^{-1}$. The calculated X-state level spacings (dashed vertical lines) are superimposed. Most unlabeled lines belong to adjacent v' groups. Solid circles indicate the calculated FCFs for decay from $3(0^+)$ to $X\ {}^1\Sigma^+$ for these two cases. The maximum FCF value in (a) is 0.11 and the maximum in (b) is 0.12. Note the shift of the FCF peak to lower v'' (smaller outer turning point) with larger PA detuning.

cation of the ground-state levels. A previously measured spacing between $v''=86$ and 87 [53] is also in excellent agreement. We note that although the $3(0^+)$ state comes from the $\mathrm{K}(4s)+\mathrm{Rb}(5p_{3/2})$ asymptote, the PA laser is tuned below the $\mathrm{K}(4s)+\mathrm{Rb}(5p_{1/2})$ asymptote, so predissociation does not occur.

The relative populations of the various X-state vibrational levels are determined by the Franck-Condon factors (FCFs) for decay of the level formed by photoassociation. We expect that as PA occurs to more deeply bound levels, with smaller outer turning points, the FCFs will favor decay to more deeply bound levels of the X state. This is indeed the case, as seen in comparing Figs. 3(a) and 3(b). The peak of the X-state distribution shifts to a lower v'' for the larger (more negative) PA detuning. If we assume that the first (resonant) step of the two-photon detection process is saturated, and that the second (ionization) step is saturated and/or structureless, then the detection spectra will be a direct measure of the relative population of X-state vibrational levels. This distribution is given by the FCFs for decay of the photoassociated level, in this case a level of the $3(0^+)$ state. These FCFs, calculated using the LEVEL program [54], are superimposed on the spectra in Figs. 3(a) and 3(b). Not only does the measured peak of the distribution shift with detuning as predicted, but the relative peak heights within each distribution actually match the FCF calculations rather well.

Using PA detunings for the $3(0^+)$ state over the range 246 to 320 cm^{-1} [measured relative to its $\mathrm{K}(4S)+\mathrm{Rb}(5P_{3/2})$ asymptote, which lies 237.60 cm^{-1} above the $\mathrm{K}(4S)+\mathrm{Rb}(5P_{1/2})$ asymptote], we observe X-state levels from $v''=86-92$, which have binding energies from 29.76 to 4.45 cm^{-1}, respectively. The highest level in the X state is predicted [52] to be $v''=98$. The molecules we detect are produced over a time interval of several milliseconds before the detection laser pulse. During this time, they are exposed to the Rb MOT trap (and repump) light, tuned near the $\mathrm{K}(4S)+\mathrm{Rb}(5P_{3/2})$ asymptote, and PA light. This could cause off-resonant reexcitation and subsequent dissociation of the X-state molecules, particularly for high v''. Such a state-dependent destruction mechanism would modify the X-state vibrational distribution from that initially produced according to the FCFs. However, we see no evidence for this alteration.

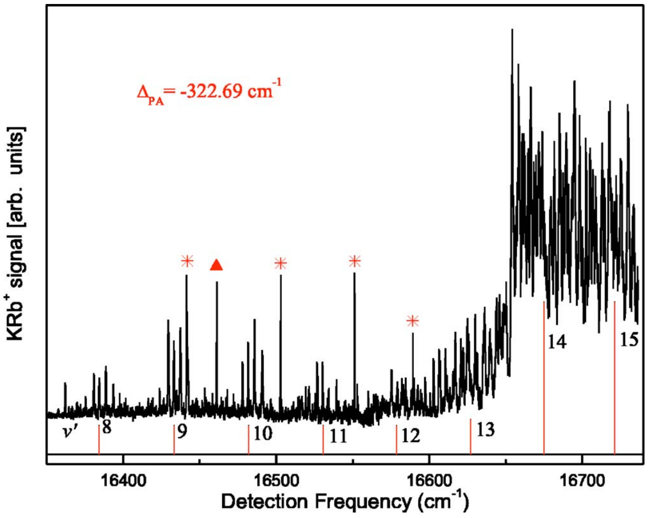

FIG. 4. (Color online) Detection spectrum for triplet molecules. The PA laser is tuned to a $3(0^-)$ $(J=1)$ level at 12 493.91 cm^{-1}, which corresponds to a detuning of $-322.69\ \mathrm{cm}^{-1}$ below the $\mathrm{K}(4S)+\mathrm{Rb}(5P_{3/2})$ asymptote. Each group of lines is labeled according to the v' level of the $4\ {}^3\Sigma^+$ state which is excited. The blue end of the spectrum becomes congested due in part to the emergence of transitions to the $3\ {}^3\Pi$ state, which have not yet been assigned. The triangle indicates a one-photon atomic transition from $\mathrm{Rb}(5p_{3/2}) \rightarrow (5f)$. Asterisks indicate two-photon transitions from $\mathrm{Rb}(5s)$ to atomic Rydberg states: $13d$, $14d$, $15d$, and $16d$ from left to right.

IV. DETECTION SPECTRA FOR TRIPLET MOLECULES

State-selective detection of triplet $a\ {}^3\Sigma^+$ molecules is carried out in a similar manner to that described above for singlet $X\ {}^1\Sigma^+$ molecules. The only difference is that the PA laser is tuned to a level which decays to the a state. For this work, we use the $3(0^-)$ state from the $\mathrm{K}(4S)+\mathrm{Rb}(5P_{3/2})$ asymptote, which correlates to the $1\ {}^3\Pi$ state at short range [26]. Higher detection laser intensities are required for comparable signal levels from triplet molecules. The triplet detection spectra are obtained over the same wavelength range, but of course involve different upper states: $4\ {}^3\Sigma^+$ and probably $3\ {}^3\Pi$. The spectroscopy of the $4\ {}^3\Sigma^+$ state, along with that of the $4\ {}^1\Sigma^+$ state (used for singlet detection), will be described in a separate publication [50]. A $\sim 400\ \mathrm{cm}^{-1}$ scan is shown in Fig. 4. The structure repeating at $\sim 50\ \mathrm{cm}^{-1}$ corresponds to the vi-

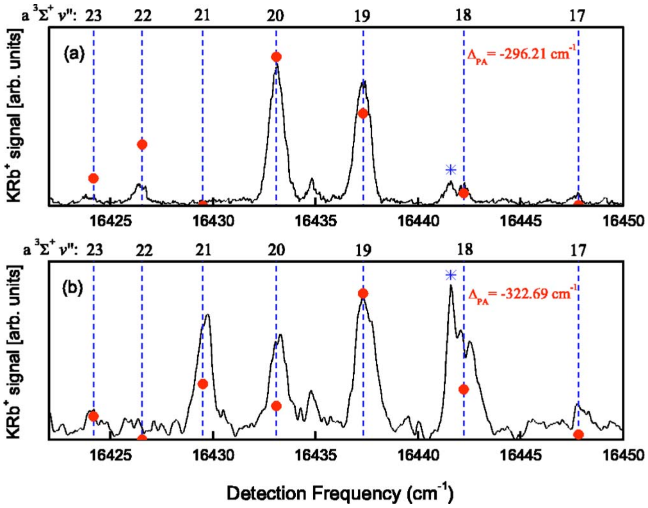

FIG. 5. (Color online) An expanded view of the $v'=9$ group of lines in the triplet detection spectrum for two different $3(0^-)$ PA detunings: (a) -296.21 and (b) -322.69 cm^{-1}. The calculated *a*-state level spacings (dashed vertical lines) are superimposed. Solid circles indicate the calculated FCFs for decay from the $3(0^-)$ state to the $a\,^3\Sigma^+$ state. The maximum FCF value in (a) is 0.10 ($v''=20$) and the maximum in (b) is 0.10 ($v''=19$). Asterisks indicate the two-photon atomic transition Rb($5s$)$\rightarrow$($13d$).

brational spacing of the $4\,^3\Sigma^+$ state. Assigned vibrational levels are indicated in the figure. The congested region of larger signal to the blue may involve the $3\,^3\Pi$ state, but specific assignments have not yet been made.

Two-photon transitions to atomic Rb Rydberg states sometimes can be seen as well in the triplet spectra, due to leakage from the space-charge-broadened Rb$^+$ TOF peak into the KRb$^+$ TOF peak. We also see ions at the Rb atomic $5p_{3/2}\rightarrow 5f$ one-photon transition. The $5p_{3/2}$ level is populated by the MOT lasers and this dipole-forbidden transition is enabled by the $\sim$160 V/cm electric field used for extraction. These atomic lines serve as useful frequency markers and verify that the laser frequency measurements are accurate to 0.16 cm^{-1}. These lines are not readily observable in the spectra of singlet molecules (Fig. 2) because lower laser intensities are used.

Figure 5 is an expanded view of the spectrum, encompassing only one vibrational level of the $4\,^3\Sigma^+$ upper state. The structure here is due to the near-dissociation levels of the $a\,^3\Sigma^+$ state. The vibrational levels show spacings of 2.4 to 5.6 cm^{-1}. Such spacings correspond to levels $v''=20$ to 26 in the *ab initio* potential of Kotochigova *et al.* [55] and $v''=18$ to 24 in the *ab initio* potentials of Park *et al.* [56] and of Rousseau *et al.* [51]. These three potentials have been compared by Zemke *et al.* [57]. However, a definitive assignment has very recently become available, based on new Fourier transform spectra [58]. This clearly indicates we have observed levels $v''=17$ to 23, as shown in Table I. To verify this assignment, we plan direct measurement of the binding energies by scanning a separate cw laser to deplete the ground-state levels. We have recently observed this "ion dip" spectroscopy for $X\,^1\Sigma^+$, $v''=89$.

As for the singlet molecules, we can use the peak heights as a measure of the lower-level ($a\,^3\Sigma^+$) populations. There is a small, but noticeable shift in the distribution to lower v'' for larger (more negative) PA detunings. Also shown in these figures are the calculated FCFs for decay from each $3(0^-)$ PA level to various levels of the $a\,^3\Sigma^+$ state. The Kotochigova *et al.* potential ($v''=20-26$) is used for these FCF calculations because it has the best long range behavior [57]. The overall locations of the distributions, including the shift with PA detuning, match the data. However, compared to the singlet spectra (Fig. 3), individual peak heights are not as accurately predicted. We hope future calculations based on the $a\,^3\Sigma^+$ potential of [58], once it is available, can give more accurate results. Linewidths in the triplet spectra are somewhat broader than those in the singlet spectra. Power broadening, spin-spin, second-order spin-orbit, rotational, and hyperfine structure should all contribute to the line shapes observed.

TABLE I. Level spacings ($\Delta G_{v+1/2}$, in cm^{-1}) in the ^{39}K^{85}Rb $a\,^3\Sigma^+$ state.

v	Fourier transform spectra	PA-R2PI (this work)
17	5.49	5.60
18	4.84	4.90
19	4.23	4.23
20	3.60	3.56
21	2.99	2.96
22	2.41	2.38

PA detunings for the $3(0^-)$ state from 244 to 323 cm^{-1} [measured relative to its K($4P$)+Rb($5P_{3/2}$) asymptote] have been used to observe *a*-state levels from $v''=17-23$. These have binding energies from 29.02 to 5.31 cm^{-1}, respectively. This numbering, based on the Fourier transform spectra in [58], is definitive because the vibrational assignment is based on two different isotopes. None of the three sets of *ab initio* potentials from [51,55,56] can give this exact numbering, although a good vibrational spacing match can be found if we adjust their numbering by one or three [57].

An important difference between singlet and triplet molecules is that the triplets have a nonzero magnetic moment and can therefore be magnetically trapped. We have previously demonstrated this trapping in the quadrupole magnetic field of the MOT [25,26] by delaying the molecule detection with respect to the turn-off of the PA laser. This difference in magnetic properties could be utilized as a singlet-triplet "filter" to distinguish the two types of molecules. We do see cases where both $X\,^1\Sigma^+$ and $a\,^3\Sigma^+$ molecules appear in the same region of the detection spectrum. An example, using PA to the $3(0^+)$ state, is shown in Fig. 6. At long range, the $3(0^+)$ state should decay to both $X\,^1\Sigma^+$ and $a\,^3\Sigma^+$ states [26], so we expect to detect both. However, the FCFs for the first step of the detection process play an important role. For high-v'' levels of $X\,^1\Sigma^+$, the overlap with $4\,^1\Sigma^+$ levels comes primarily from the outer turning point. On the other hand, overlap of high-v'' levels of $a\,^3\Sigma^+$ with $4\,^3\Sigma^+$ levels comes primarily from the inner turning point and becomes more favorable in the lower-energy region of the spectrum. The overall detection efficiencies (including the ionization step) for $X\,^1\Sigma^+$ and $a\,^3\Sigma^+$ become comparable in the region shown

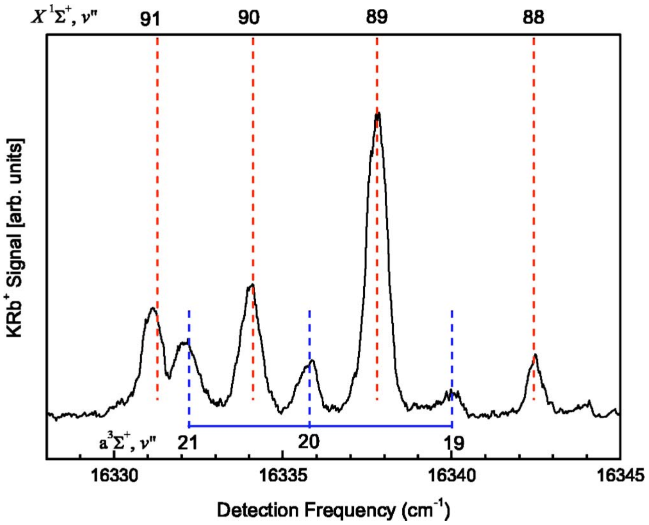

FIG. 6. (Color online) Detection spectrum with overlapping singlet and triplet features. The PA laser is tuned to a $3(0^+)$ $(J=1)$ level at a detuning of -246.66 cm^{-1} below the $K(4S)+Rb(5P_{3/2})$ asymptote. $X\,^1\Sigma^+$ molecules are detected through $4\,^1\Sigma^+$ $(v'=33)$, while $a\,^3\Sigma^+$ molecules are detected through $4\,^3\Sigma^+$ $(v'=4)$. Expected singlet and triplet line positions are indicated.

in Fig. 6. Although we do see triplet features in a primarily singlet detection spectrum [using PA to $3(0^+)$], we do not see singlet features in the triplet detection spectra [using PA to $3(0^-)$]. This is consistent with the fact that at long range, $3(0^+)$ can decay to both $X\,^1\Sigma^+$ and $a\,^3\Sigma^+$ states, while $3(0^-)$ can decay only to $a\,^3\Sigma^+$ [26].

V. CONCLUSIONS

In summary, we have realized vibrationally state-selective detection of near-dissociation levels of ultracold KRb molecules in the $X\,^1\Sigma^+$ ground state and the $a\,^3\Sigma^+$ metastable state. This state selectivity will be crucial to future experiments in ultracold molecular collisions and reactions where specific initial and final states must be measured. This capability is equally important in diagnosing population transfer, e.g., from high to low v'' [19]. In fact, the first step in our singlet detection $(4\,^1\Sigma^+ \leftarrow X\,^1\Sigma^+)$ is a good candidate for realizing this type of transfer. As an example, if we start in $X\,^1\Sigma^+$ $(v''=89)$, the FCF for excitation to $4\,^1\Sigma^+$ $(v'=40)$ is quite large (0.02) due to overlap at the outer turning points. On the other hand, overlap at the inner turning points gives a favorable FCF of ~ 0.01 for decay (or stimulated emission) of $4\,^1\Sigma^+$ $(v'=40)$ to the absolute ground state $X\,^1\Sigma^+$ $(v''=0)$. These large FCFs indicate that coherent two-photon transfer, such as Stimulated Raman adiabatic passage (STIRAP) [59], should be feasible with narrow-linewidth quasi-cw lasers.

The two-photon, one-color detection we have employed is particularly convenient because only one tunable laser is required. However, the second (ionizing) step generally requires high intensity, resulting in power broadening of the first (bound-bound) step. Two-photon, two-color detection [e.g., through states from the $K(4s)+Rb(5p)$ asymptotes] may offer some benefits. The ionizing step can be driven with high intensity from a fixed-frequency pulsed laser, such as a frequency-doubled YAG laser. If the first step is driven with a narrow-linewidth cw laser at low intensity, rotational resolution should be achievable.

ACKNOWLEDGMENTS

We gratefully acknowledge support from NSF and the University of Connecticut Research Foundation. We thank Chad Orzel for making the pulsed dye laser available, and Ye Huang and Hyewon K. Pechkis for laboratory assistance.

[1] J. T. Bahns, P. L. Gould, and W. C. Stwalley, Adv. At., Mol., Opt. Phys. **42**, 171 (2000).

[2] F. Masnou-Seeuws and P. Pillet, Adv. At., Mol., Opt. Phys. **47**, 53 (2001).

[3] H. L. Bethlem and G. Meijer, Int. Rev. Phys. Chem. **22**, 73 (2003).

[4] *Ultracold Polar Molecules: Formation and Collisions*, Special issue of Eur. Phys. J. D **31**, 149 (2004), edited by J. Doyle, B. Friedrich, R. V. Krems, and F. Masnou-Seeuws.

[5] L. Santos, G. V. Shlyapnikov, P. Zoller, and M. Lewenstein, Phys. Rev. Lett. **85**, 1791 (2000).

[6] S. Yi and L. You, Phys. Rev. A **61**, 041604(R) (2000).

[7] K. Goral, K. Rzazewski, and T. Pfau, Phys. Rev. A **61**, 051601(R) (2000).

[8] K. Goral and L. Santos, Phys. Rev. A **66**, 023613 (2002).

[9] B. Damski, L. Santos, E. Tiemann, M. Lewenstein, S. Kotochigova, P. Julienne, and P. Zoller, Phys. Rev. Lett. **90**, 110401 (2003).

[10] K. Goral, L. Santos, and M. Lewenstein, Phys. Rev. Lett. **88**, 170406 (2002).

[11] M. A. Baranov, M. S. Marenko, V. S. Rychkov, and G. V. Shlyapnikov, Phys. Rev. A **66**, 013606 (2002).

[12] D. DeMille, Phys. Rev. Lett. **88**, 067901 (2002).

[13] M. G. Kozlov and L. N. Labzowsky, J. Phys. B **28**, 1933 (1995).

[14] J. L. Bohn, Phys. Rev. A **63**, 052714 (2001).

[15] E. Bodo and F. A. Gianturco, J. Chem. Phys. **116**, 9222 (2002).

[16] N. Balakrishnan and A. Dalgarno, Chem. Phys. Lett. **341**, 652 (2001).

[17] W. C. Stwalley and H. Wang, J. Mol. Spectrosc. **195**, 194 (1999).

[18] A. J. Kerman, J. M. Sage, S. Sainis, T. Bergeman, and D. DeMille, Phys. Rev. Lett. **92**, 153001 (2004).

[19] J. M. Sage, S. Sainis, T. Bergeman, and D. DeMille, Phys. Rev. Lett. **94**, 203001 (2005).

[20] T. Bergeman, A. J. Kerman, J. Sage, S. Sainis, and D. DeMille, Eur. Phys. J. D **31**, 179 (2004).

[21] M. W. Mancini, G. D. Telles, A. R. L. Caires, V. S. Bagnato, and L. G. Marcassa, Phys. Rev. Lett. **92**, 133203 (2004).

[22] J. P. Shaffer, W. Chalupczak, and N. P. Bigelow, Phys. Rev. Lett. **82**, 1124 (1999).

[23] C. Haimberger, J. Kleinert, M. Bhattacharya, and N. P. Bigelow, Phys. Rev. A **70**, 021402(R) (2004).

[24] H. Wang, Bull. Am. Phys. Soc. **48**, J1.025 (2003).

[25] D. Wang, J. Qi, M. F. Stone, O. Nikolayeva, H. Wang, B. Hattaway, S. D. Gensemer, P. L. Gould, E. E. Eyler, and W. C. Stwalley, Phys. Rev. Lett. **93**, 243005 (2004).

[26] D. Wang, J. Qi, M. F. Stone, O. Nikolayeva, B. Hattaway, S. D. Gensemer, H. Wang, W. T. Zemke, P. L. Gould, E. E. Eyler, W. C. Stwalley, Eur. Phys. J. D **31**, 165 (2004).

[27] J. Herbig, T. Kramer, M. Mark, T. Weber, C. Chin, H. C. Nägerl, and R. Grimm, Science **301**, 1510 (2003).

[28] C. Chin, A. J. Kerman, V. Vuletic, and S. Chu, Phys. Rev. Lett. **90**, 033201 (2003).

[29] S. Dürr, T. Volz, A. Marie, and G. Rempe, Phys. Rev. Lett. **92**, 020406 (2004).

[30] K. Xu, T. Mukaiyama, J. R. Abo-Shaeer, J. K. Chin, D. E. Miller, and W. Ketterle, Phys. Rev. Lett. **91**, 210402 (2003).

[31] S. Jochim, M. Bartenstein, A. Altmeyer, G. Hendl, S. Riedl, C. Chin, J. H. Denschlag, and R. Grimm, Science **302**, 2101 (2003).

[32] J. Cubizolles, T. Bourdel, S. J. J. M. F. Kokkelmans, G. V. Shlyapnikov, and C. Salomon, Phys. Rev. Lett. **91**, 240401 (2003).

[33] K. E. Strecker, G. B. Partridge, and R. G. Hulet, Phys. Rev. Lett. **91**, 080406 (2003).

[34] M. W. Zwierlein, C. A. Stan, C. H. Schunck, S. M. F. Raupach, S. Gupta, Z. Hadzibabic, and W. Ketterle, Phys. Rev. Lett. **91**, 250401 (2003).

[35] C. A. Regal, C. Ticknor, J. L. Bohn, and D. S. Jin, Nature (London) **424**, 47 (2003).

[36] M. Greiner, C. A. Regal, and D. S. Jin, Nature (London) **426**, 537 (2003).

[37] C. A. Stan, M. W. Zwierlein, C. H. Schunck, S. M. F. Raupach, and W. Ketterle, Phys. Rev. Lett. **93**, 143001 (2004).

[38] S. Inouye, J. Goldwin, M. L. Olsen, C. Ticknor, J. L. Bohn, and D. S. Jin, Phys. Rev. Lett. **93**, 183201 (2004).

[39] Y. B. Band and P. S. Julienne, Phys. Rev. A **51**, R4317 (1995).

[40] S. Kotochigova, E. Tiesinga, and P. S. Julienne, Eur. Phys. J. D **31**, 189 (2004).

[41] W. C. Stwalley, Eur. Phys. J. D **31**, 221 (2004).

[42] A. N. Nikolov, J. R. Ensher, E. E. Eyler, H. Wang, W. C. Stwalley, and P. L. Gould, Phys. Rev. Lett. **84**, 246 (2000).

[43] C. Gabbanini, A. Fioretti, A. Lucchesini, S. Gozzini, and M. Mazzoni, Phys. Rev. Lett. **84**, 2814 (2000).

[44] A. Fioretti, C. Amiot, C. M. Dion, O. Dulieu, M. Mazzoni, G. Smirne, and C. Gabbanini, Eur. Phys. J. D **15**, 189 (2001).

[45] M. Kemmann, I. Mistrik, S. Nussmann, H. Helm, C. J. Williams, and P. S. Julienne, Phys. Rev. A **69**, 022715 (2004).

[46] Y. Huang, H. K. Pechkis, J. Qi, D. Wang, E. E. Eyler, P. L. Gould, and W. C. Stwalley (unpublished).

[47] C. M. Dion, O. Dulieu, D. Comparat, W. de Souza Melo, N. Vanhaecke, P. Pillet, R. Beuc, S. Milosevic, and G. Pichler, Eur. Phys. J. D **18**, 365 (2002).

[48] A. N. Nikolov, E. E. Eyler, X. T. Wang, J. Li, H. Wang, W. C. Stwalley, and P. L. Gould, Phys. Rev. Lett. **82**, 703 (1999).

[49] F. K. Fatemi, K. M. Jones, P. D. Lett, and E. Tiesinga, Phys. Rev. A **66**, 053401 (2002).

[50] D. Wang, E. E. Eyler, P. L. Gould, and W. C. Stwalley (unpublished).

[51] S. Rousseau, A. R. Allouche, and M. Aubert-Frécon, J. Mol. Spectrosc. **203**, 235 (2000).

[52] W. Zemke and W. C. Stwalley, J. Chem. Phys. **120**, 88 (2004).

[53] C. Amiot and J. Vergès, J. Chem. Phys. **112**, 7068 (2000).

[54] R. J. LeRoy, University of Waterloo Chemical Physics Research Report CP-642R (unpublished), web site http://leroy.uwaterloo.ca

[55] S. Kotochigova, P. S. Julienne, and E. Tiesinga, Phys. Rev. A **68**, 022501 (2003).

[56] S. J. Park, Y. J. Choi, Y. S. Lee, and G. H. Jeung, Chem. Phys. **257**, 135 (2000).

[57] W. Zemke, R. Côté, and W. C. Stwalley, Phys. Rev. A **71**, 062706 (2005).

[58] E. Tiemann and O. Docenko (private communication).

[59] K. Bergmann, H. Theuer, and B. W. Shore, Rev. Mod. Phys. **70**, 1003 (1998).